# CHARACTERIZATION OF AND CORRECTION FOR CULTURAL NOISE

ANDREAS JUNGE
*Institut für Meteorologie und Geophysik, Universität Frankfurt am Main, Feldbergstr. 47, D-60323 Frankfurt/Main, Germany*

**Abstract.** Surveys of time varying electromagnetic fields result in time series consisting of signals and noise, the latter defined as that part of the data which cannot be explained by a theory. Man-made contributions to noise can be subdivided into active and passive sources and are complex in character. As Szarka has treated this topic extensively in a recent review paper (Szarka, 1988), only a few further examples are presented here.

Following discussion of noise correction in transient electromagnetic investigations which consists mainly of sophisticated stacking and filter procedures, several aspects of its correction in magnetotelluric and geomagnetic depth sounding data are considered. These include:

a) The methods of treatment of single time series in the presence of visible noise – its detection, removal and sometimes replacement by data predicted from undisturbed intervals.
b) The investigation of time series interrelations. This is mainly coherence based and – if possible – takes advantage of remote reference techniques.
c) The examination of the statistical properties of the time series by regression analysis. This leads to the weighting of time segments of data in order to achieve unbiased and minimum variance estimates based on identically and independently Gaussian distributed residuals.
d) The application of constraints. These can further improve the estimates' quality.
e) The use of simultaneously recorded multistation data. This can contribute remarkably to noise suppression as well as to the treatment of non-uniform source fields.
f) Leveraging and confidence limits. Problems relating to the former have not yet been solved satisfactorily while the Jacknife method seems to be an easy way of determining the latter.

Thanks to the modern processing techniques reviewed in this paper it should be possible to obtain a rather dense net of high quality data in spite of the world-wide increasing noise level. As most processing codes are widely accessible current problems are more related to availability of instruments, carrying out the measurements and reserving enough time for thorough data processing.

**Key words:** Cultural noise, electromagnetic induction, data processing, time series analysis

## 1. Introduction

Electromagnetic surveys depend on the recording of accurate signals which are generally contaminated by noise. In the following, noise is defined as that part of the data which cannot be explained by the framework of a theory. In the case of electromagnetic induction measurements, theory implies consistent relationships between simultaneously observed components of the magnetic and electric field.

The sources of electromagnetic noise differ substantially, as follows:

a) The theory applied may be inadequate for the real study, e.g. the assumption of a plane wave or of a homogeneous electric field between telluric electrodes.

*Surveys in Geophysics* **17:** 361–391, 1996.

b) Instrumental noise, e.g. sensor noise due to temperature dependence of magnetometers or to electrochemical processes in the telluric electrodes (Petiau and Dupis, 1980; Junge, 1990) and faults in the analog or digital recording devices.

c) Environmental noise defined as all natural electric and magnetic fields of no interest to conductivity studies, e.g. the impact of weather conditions, seismic noise as far as sensor motion is concerned (Nichols *et al.*, 1988), biological noise which might result from electrochemical processes in plants (Morat *et al.*, 1994) and oceanic noise related to the movement of seawater in the earth's magnetic field (cf. Larsen, 1992).

d) Cultural or man-made noise may be subdivided into active and passive noise, the former being due to primary sources while the latter refers to induced secondary fields, e.g. grounded pipelines, fences, etc.

Although it is sometimes difficult and not of particular interest to separate the different types of noise, it is the last category which is the main topic of this review. It is considered from both practical and theoretical points of view, with emphasis on various methods for noise correction. There is also some initial discussion of the characterization of noise as it might help reduce its influence considerably.

## 2. Characterization of Cultural Noise

As this topic has been treated extensively in a recent review paper (Szarka, 1988) only some aspects will be presented.

The main sources of cultural noise are all electric power consuming devices. e.g. electric trains, power stations and lines, mining areas, electric fences, radio and television transmitters, corrosion protected pipelines, etc. In highly populated areas the noise energy is very often polarized and exceeds the natural signal several times. A variety of examples of cultural noise, including the influence of mining and of an unbalanced power network, is given by Adam *et al.* (1986), further respectively three examples are chosen here to illustrate specific noise of well known origin. The first two refer to stationary and non-stationary noise while the last one demonstrates the impact of a moving source.

Figure 1 shows the effect of a corrosion protected pipeline on the magnetic field components, measured at two sites located on a low conductivity granitic area. Sites VOH1 and VOH2 are 90 and 490 m from the pipeline. The effect is seen only in $B_z$, the decrease in signal with increasing distance reflecting very well the inverse distance law for a line current. The electric current in the pipeline can be clearly identified as the signal source, as a result of the two sites comparison.

Figure 2 demonstrates the effect of a mobile military radar transmitter on the magnetic field components of an MT (= magnetotelluric) record. The sequence of sweeps coincides with the rotation of the radar antenna, the frequency being the pulse frequency – usually above 100 Hz – not that of the radar signal. With regard to $B_x$ being roughly twice as large as $B_z$ and the absence of the signal in the electric

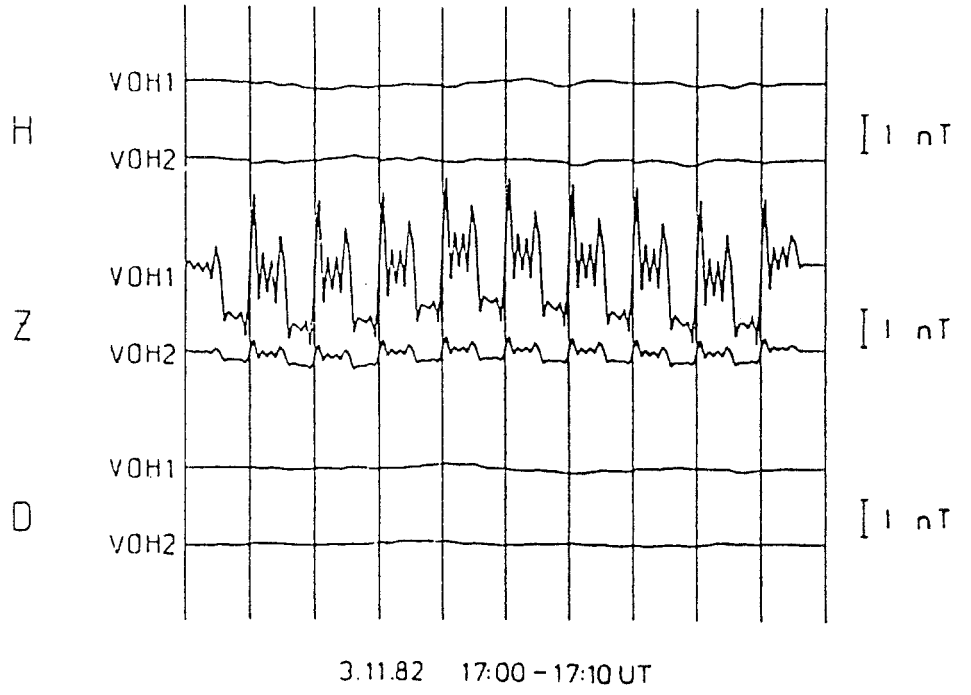


*Figure 1.* 10 min interval of magnetic field variations ($H \equiv B_x$, $D \equiv B_y$, $Z \equiv B_z$) at two sites in 90 m (VOH1) and 490 m (VOH2) distance from a corrosion protected pipeline (Brasse and Junge, 1984).

field, the source is equivalent to a magnetic dipole with a magnetic moment vector pointing slightly upwards into the sky (cf. Li and Pedersen (1991)).

Figure 3 shows the impact of a ship moving past a sea bottom magnetometer placed at 70 m water depth. The large spike of about 160 nT amplitude and 1 min width reveals that sea traffic might severely disturb offshore experiments.

Two high resolution spectra from sites near to and 30 km distant from Göttingen are shown in Figure 4 covering the low energy range of natural excitation (Füllekrug, 1994). Both spectra show the dominant "railway" peak at 16 2/3 Hz rising up to 60 dB above the continuum, but more importantly reveal subharmonics at 12.5 and 6.25 Hz of the 50 Hz power supply in the Göttingen spectrum. The latter probably originate from phase sensitive voltage control of electrical generators, heating facilities, etc. They cannot be detected in the spectrum of Silberborn which is situated relatively far from any industrialized area and show clearly the natural signal at the first two Schumann resonance frequencies. The comparably inconspicuous Schumann resonance signal in the Göttingen spectrum reflects the enhanced level of presumably broadband industrial noise there.

Several attempts have been made to use industrial noise for the investigation of conductivity structures. Ádám *et al.* (1989) tried to map the electrical conductance in the Komló coal field mining area but the investigations were aggravated by

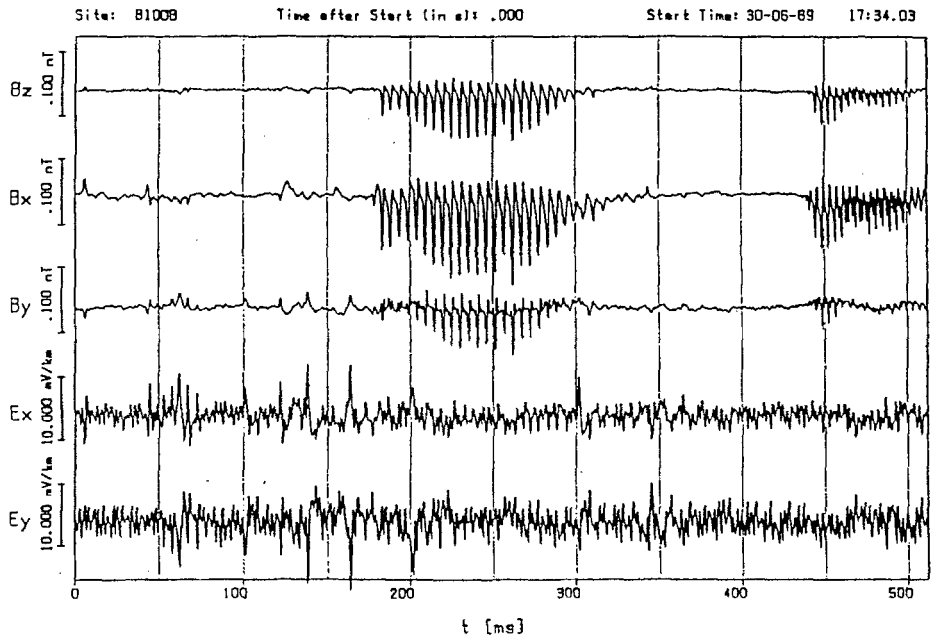


*Figure 2.* 512 ms interval of MT time series containing two radar sweeps (Brasse, 1993).

variation of the source field location with time and by uncertainties of the source mechanism.

If the noise source can be regarded as fixed, e.g. being far enough from the recording site, the transfer functions may be divided into near and far field parts according to the frequency-skindepth relation. The 45° slope of the $\log \rho_a - \log T$ curve accompanied by zero phase and unit tipper magnitude for the lower frequencies is characteristic of near field transfer functions.

The occurrence of these features guided Masero and Fontes (1992) to map the transition between sediments and the basement of the Colônia impact structure, Brazil. Cultural noise originating in São Paulo dominated the response functions where the resistive basement influenced the diffusion process. However, the noise was shielded elsewhere by the conductive sediments and thus natural signals could be detected up to certain period above the sediments.

Qian and Pedersen (1991) even succeeded in modelling the near/far field response functions obtained in the industrial Tangshan Area, China (Figure 5). They applied a controlled source formulation and took advantage of the property that the resulting impedance tensors are independent of the dipole orientation.

As man-made electromagnetic noise resembles in many aspects the features of controlled source electromagnetics, some basic studies of this topic are of high value (cf. Goldstein and Strangeway (1975), Bartel and Jacobson (1987), Bartel and Becker (1988)). Buried or grounded conductors such as metal pipes, cables,

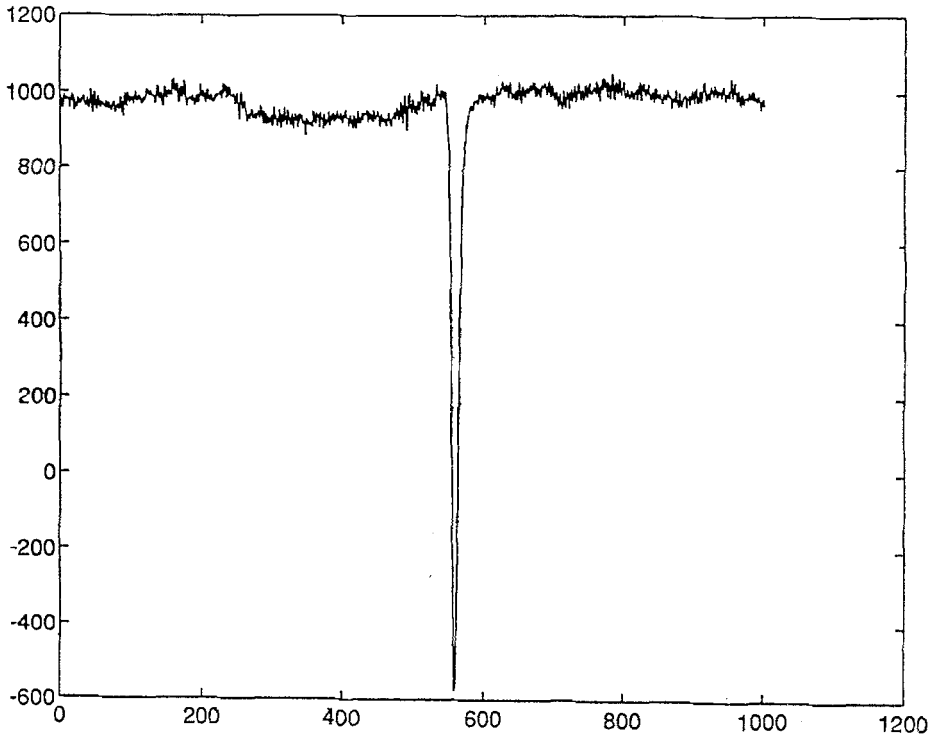


*Figure 3.* Magnetic field component recorded on the sea bottom at 70 m depth demonstrating the effect of a ship passing by (Filloux *et al.*, 1994). The vertical axis shows the magnetic field in 1/10 nT, the time axis sample numbers ($\Delta t = 1/2048h \approx 1.8s$).

electric fences, etc. might severely distort results obtained from electromagnetic measurements. As far as they are not the major target of the investigation they can be regarded as culturally induced noise. As such passive noise does not vary with time it can only be reduced by careful model studies but these are often hampered by lack of knowledge of the real status of the earthing, resistance and location.

While Ogunade (1986) treats analytically the response of a line conductor buried in horizontally stratified media with respect to various source fields, numerical approaches may be used in more general cases. Qian and Boerner (1995) model an uncoated line conductor buried in a 1-D structure using an integral equation. The major parameters are the longitudinal resistance of the conductor and its galvanic and inductive coupling with the surrounding earth. The same authors investigate numerically the influence of grounded circuit elements on electromagnetic response functions, especially at high frequencies when the skin depth is shorter than the circuit length between adjacent grounding points (Qian and Boerner, 1994). They claim that their numerical models may easily be generalized in terms of more com-

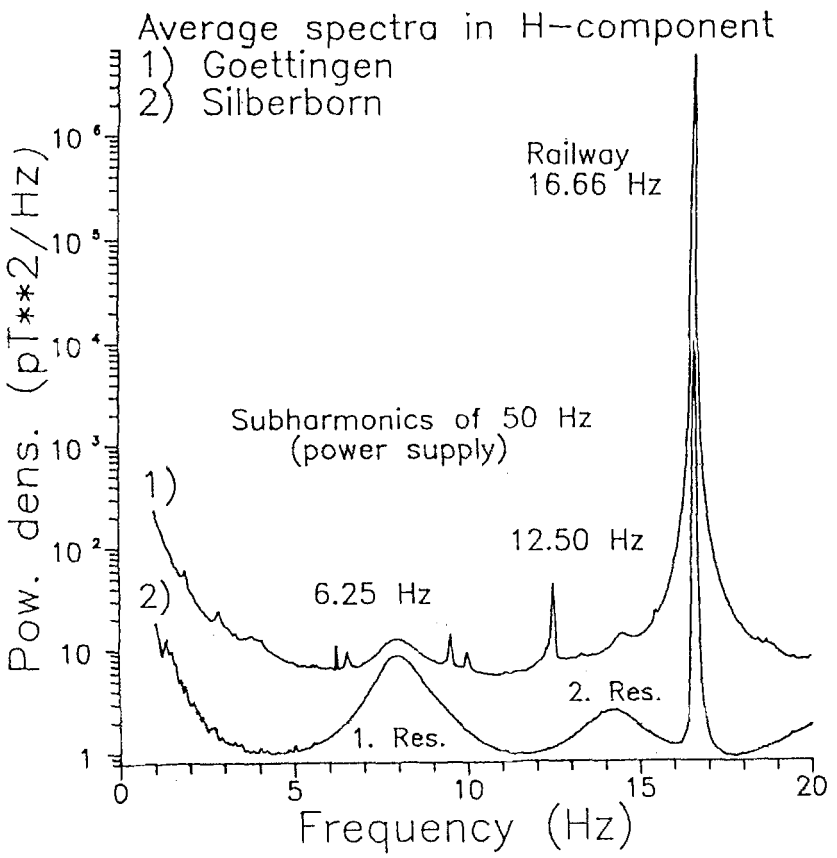


*Figure 4.* High resolution spectra of the $B_x$ component at two sites, one near Göttingen and the other at 30 km distance (Silberborn) for the frequency range between 1 and 20 Hz (Füllekrug, 1994).

plicated source field and conductivity structures and thus provide a useful tool for both characterization of and correction for noise.

## 3. Correction for Noise

Correction for noise is tackled by a large number of methods ranging from visual inspection of time series, through empirical criteria, to highly sophisticated investigations of the statistical properties of noise. Due to the advances in recording techniques, digital data have superseded analog recordings. However, Ádám *et al.* (1986) point out that, in areas of high noise level, analog recordings will show high frequency noise which might not be suppressed sufficiently by anti-alias filters.

It seems now to be generally accepted that visual inspection of time series should not be replaced completely by automatic processing techniques. On the other hand the purely visual selection of "good" data is – especially for the high frequency

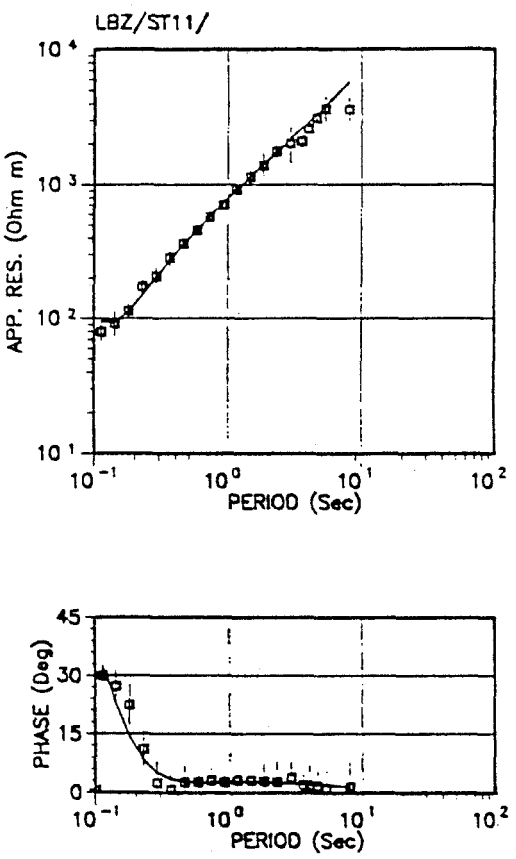


*Figure 5.* MT transfer functions $\rho_a$ and $\phi$ at a site in the industrial Tangshan Area, China. Model response for a controlled source formulation with transmitter-receiver separation of 18 km (Qian and Pedersen, 1991).

bands – time consuming and thus cost-intensive, and hidden noise of low energy but of frequent occurrence might be severely distorting the data. The latter feature concerns any frequency range and appears more often than assumed in the past.

In general the aim of any processing scheme is the selection of a set of statistically independent data with a known distribution of noise. It might be approached to a certain extent by prewhitening, tapering, filter, smoothing and weighted stacking procedures. These techniques are described by a large number of textbooks (e.g. Jenkins and Watts, 1968; Bendat and Piersol, 1971; Otnes and Enochson. 1972; Papoulis, 1987).

The algorithm for deriving the estimate from a given data set is called the estimator. Estimates are generally characterized by a systematic deviation from the true value (bias) and by a random deviation. The optimum choice of the estimator depends on the assumed physical and statistical properties of the observed quantitities. Both properties may vary with time (non-stationarity). The dilemma

encountered with all processing schemes is not the intrinsic uncertainty of randomly distributed data but the problem of finding the right estimator for the actual data.

The estimation algorithm yielding the estimate with minimum variance is efficient. If it is insensitive to outliers, i.e. deviations from the assumed sample distribution, it is called robust. The relative number of outliers, i.e. the order of the distributional deviation at which the estimator fails to be insensitive, is called its break down point. A reasonable estimator should be efficient and robust with a high breakdown point. For automatic schemes the maximum breakdown point is 0.5 which means that more than 50% of the data must fulfill the basic assumptions. For example in Figure 2 only the gaps between the radar sweeps are useful for the interpretation. If the ratio of the sweep length to the gap length exceeds one, additional constraints have to be introduced to ensure that an automatic algorithm is robust. Comparing different algorithms therefore needs careful inspection for any "hidden" constraints.

Robust methods have been used intuitively for as long as judgement on statistical basis has existed but it was not before Huber's study (1964) that this subject has been given a generalized mathematical treatment. A rather theoretical survey has been given by Huber (1981), but a more comprehensible introduction has been provided by Hampel *et al.* (1986). Only very recently the ideas of robust parameter estimation have been introduced to geophysical electromagnetic processing methods (cf. Egbert and Booker, 1986).

In the following section some processing methods employed in active transient electromagnetic sounding will be presented followed by MT and geomagnetic depth sounding (= GDS) processing techniques.

### 3.1. Transient electromagnetic (TEM) data processing

Several noise processing techniques are compared by Macnae *et al.* (1984) with specific emphasis on the time domain UTEM 3 system. They consist basically of successive stacking, sometimes with limited outlier rejection.

For the central loop configuration above a horizontally layered earth only $B_z$ contains the TEM signal while $B_x$ and $B_y$ contain the noise. Especially low frequency noise in $B_z$ can be predicted from the horizontal magnetic time series using a local noise prediction filtering technique (Spies, 1988). With a three-point prediction filter an improvement in the signal-to-noise ratio of about a factor of five can be achieved. Limitations of the method occur in areas with large lateral conductivity variations as the horizontal components will then contain non-neglibible parts of the signal.

Long Offset Transient Electromagnetic Methods (LOTEM) require the precise determination of the baseline and the signal amplitude. As stacking procedures often cannot cope satisfactorily with periodic and sporadic noise, Strack *et al.* (1989) have presented the application of a prestack recursive true amplitude notch filter. The filter has to be applied before stacking as only then possible phase

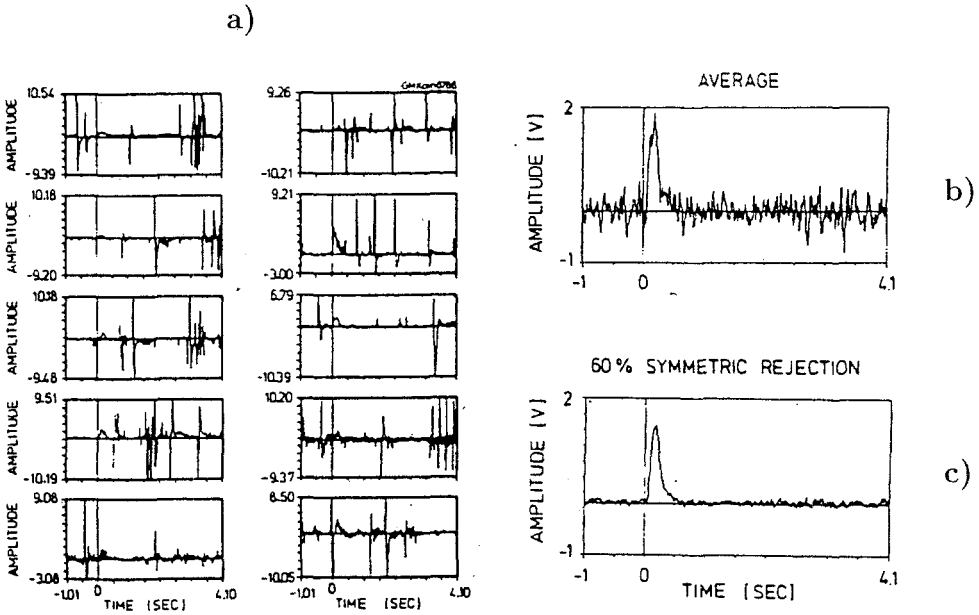


*Figure 6.* TEM processing: (a) 10 raw transient contaminated with sporadic noise. (b) Stacked without and (c) with $\alpha = 60\%$ rejection (Strack *et al.*, 1989).

instabilities of the periodic noise can be considered. The influence of sporadic noise is eliminated to a certain extent by selective stacking. The data of every time sample are ordered and $\alpha/2\%$ of the data are rejected symmetrically at each side of the distribution. This procedure is very similar to the $\alpha$-trimmed mean, thus being robust with break-point $\alpha$. Figure 6a gives an example of transients contaminated by sporadic noise, Figure 6b describes the effect of stacking and Figure 6c that of 60% symmetric rejection.

If the noise is highly correlated further improvement is achieved using simultaneous recordings at a base site and several mobile sites. Due to long recordings a highly accurate base site transient is evaluated and subtracted from the actual time series. The residual, possibly correlated noise, can then be subtracted from each single simultaneously recorded transient at the mobile sites (Stephan and Strack, 1991).

A more sophisticated approach treats nonstationary noise using an adaptive filter technique (Olsen and Hohmann, 1992). It uses the horizontal magnetic components at a remote site to predict the noise at the primary site by a 2 point (per component) least-mean-square adaptive filter. Compared to simple subtraction noise reduction of a factor of two is achieved.

## 3.2. MT/GDS DATA PROCESSING

Correction for noise in MT/GDS processing can be roughly divided into treatment of single time series, the investigation of time series interrelations, analysis of the noise distribution and inclusion of physical constraints. It finally results in the construction of confidence limits for the estimated parameters.

### 3.2.1. *Treatment of Time Series*

In this context the treatment of time series applies to the reduction of noise of known origin. For example most data acquisition systems incorporate notch filters, generally centered at 16 2/3 Hz, 50 Hz or 60 Hz, to attenuate the most common noise source in industrialized areas. However, non-sinussoidal noise often produces significant higher harmonics which can be successfully suppressed by a delay line filter (Schnegg and Fischer, 1980). The filter is simply implemented as it corresponds to the linear difference equation

$$y_i = x_i - x_{i-n} \tag{1}$$

where $x_i$ and $y_i$ are the input and output values and $n$ is the lag depending on the sampling rate and the harmonics to be suppressed. Figure 7 demonstrates the effect of the application of 16 2/3 and 50 Hz delay line filters to noise contaminated data. Figure 7a shows the filter response which is highly non-linear and thus should be applied only if necessary; in MT/GDS analysis, however, all spectra are similarily distorted by the filter and therefore the ratio of the spectra should not be influenced. Figure 7b presents, with very different vertical scales, an application of the filter to two contaminated time series – the periodic noise is suppressed completely! The impact of the filter on transfer function estimation in another study is shown in Figure 8a. Before filtering typical noise contaminated behaviour occurs, after filtering the shape of the curves changes completely, revealing the formerly hidden conductivity structure.

Irregular noise is only recognizable in the time series if its amplitude exceeds the natural signal. Attempts have been made by Fontes *et al.* (1988) to predict contaminated sections of the time series by a maximum entropy extension. Forward and backward prediction errors are estimated from the subset of the non-contaminated data using the Burg algorithm and then the gaps in the data are filled with averages of the estimates. Figure 8b shows that the method might lead to a considerable change in the shape of the transfer function.

### 3.2.2. *Interrelation between time series*

If the noise is not directly visible, separation of signal and noise is only possible by deriving relations between simultaneously recorded time series. The complex valued MT relations in the frequency domain are

$$\mathbf{E} = \mathbf{BZ} + \mathbf{R} \tag{2}$$

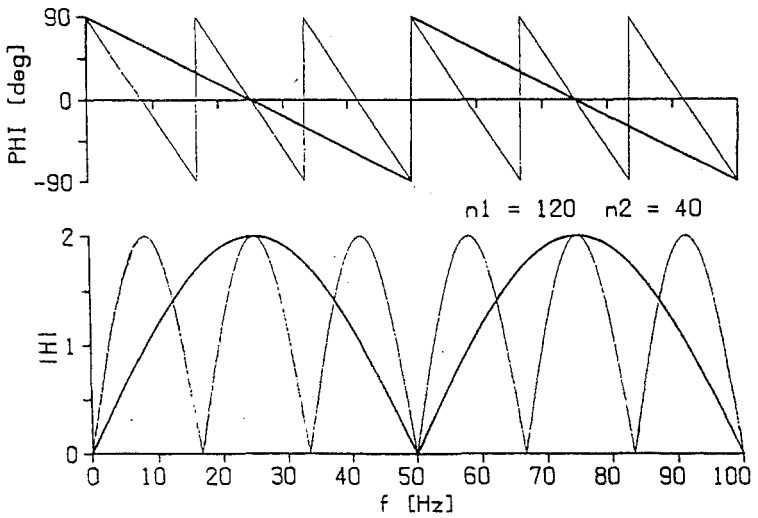


a)

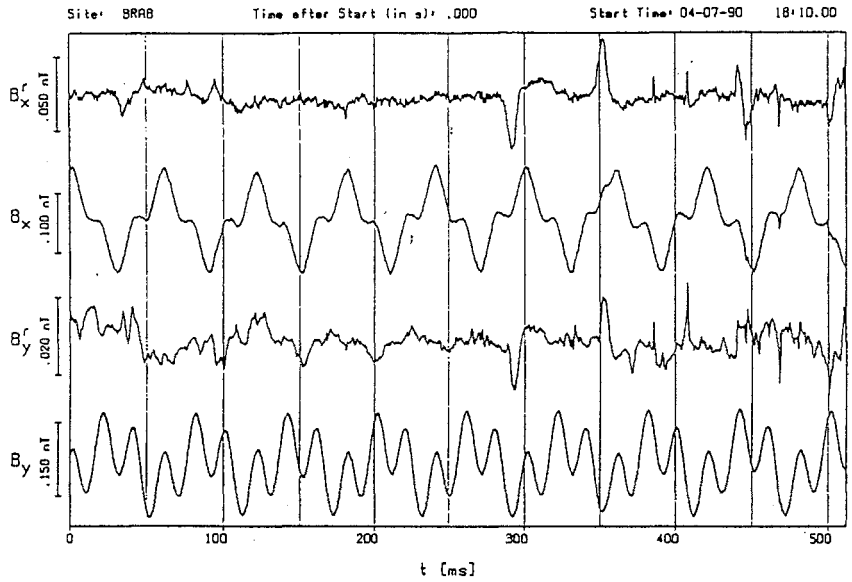


b)

*Figure 7.* Application of a delay line filter (Brasse, 1993): (a) Amplitude and phase response for 16 2/3 and 50 Hz filter, sample rate 2 kHz, $n$(16 2/3 Hz) = 120, $n$(50 Hz) = 40 (cf. (1)). (b) Unfiltered $(B_x, B_y)$ and filtered $(B_x^r, B_y^r)$ time series.

with **E** the electric and **B** the magnetic field, **Z** the impedance and **R** the residual. **E** and **R** are vectors for $J$ frequencies referring to the respective horizontal electric field component, **B** usually contains the horizontal magnetic field components and

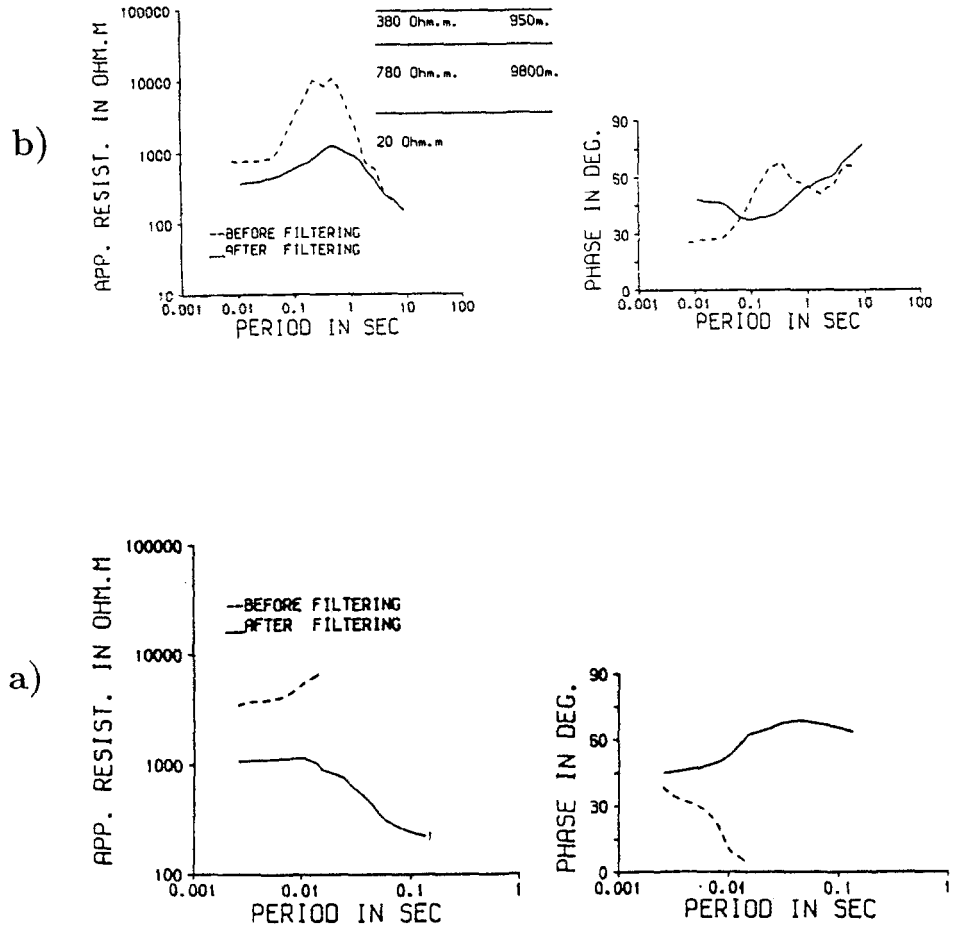


*Figure 8.* Comparison of transfer function estimates (Fontes *et al.*, 1988) $\rho_a$ and $\phi$ before (dashed) and after (solid) the application of (a) a delay line filter, (b) the maximum entropy extension (different data set!).

is a $J \times 2$ matrix, $\mathbf{Z}$ is a $2 \times J$ matrix. For example band average estimates of the transfer functions are obtained by minimizing $|\mathbf{R}|^2$,

$$\mathbf{Z} = (\mathbf{B}^H\mathbf{B})^{-1}(\mathbf{B}^H\mathbf{E}), \tag{3}$$

where $H$ is the Hermite transpose. Let the electric and magnetic fields be divided into signal and noise contributions, $\mathbf{E} = \mathbf{E}_s + \mathbf{E}_n$ and $\mathbf{B} = \mathbf{B}_s + \mathbf{B}_n$. (3) reveals that a significant $\mathbf{B}_n$ or correlation between $\mathbf{B}_n$ and $\mathbf{E}_n$ will bias the estimate of $\mathbf{Z}$.

The interchange of $\mathbf{B}$ and $\mathbf{E}$ in (3) yields an estimate for the admittance matrix from which alternatively impedance estimates can be derived. If the correlation between $\mathbf{E}_n$ and $\mathbf{B}_n$ can be neglected, (3) implies that the impedance estimates

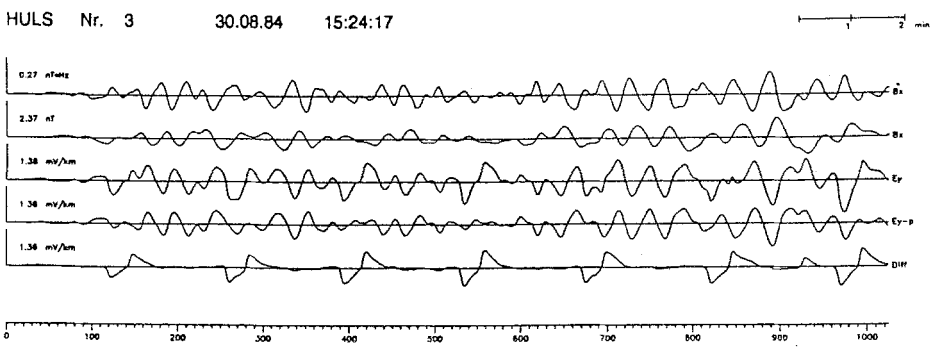


*Figure 9.* Hidden noise in the telluric field $E_y$ at a field site in Germany (Theissing, 1988). $\dot{B}_x$ and $E_y$ measured field components, $B_x$ integrated magnetic field, $E_{y-p}$ predicted electric field, Diff = $E_y - E_{y-p}$.

will be downward biased whereas the admittance estimates will be upwardbiased (cf. Sims *et al.*. 1971). However. there is no direct way to derive separate noise properties from both estimates.

If simultaneous time series at a remote site are available,

$$\mathbf{Z}_r = (\mathbf{B}_r^H \mathbf{B})^{-1} (\mathbf{B}_r^H \mathbf{E}) \tag{4}$$

with the index $r$ denoting the field at the remote site, will also yield an estimate of $\mathbf{Z}$. $\mathbf{Z}_r$ is unbiased as long as $\mathbf{B}_{rs}$ and $\mathbf{B}_s$ are correlated, $\mathbf{B}_{rn}^H \mathbf{B}_n \approx 0$ and $\mathbf{B}_{rn} \mathbf{E}_n \approx 0$. Furthermore significant bias might occur due to source field polarization (Pedersen and Svennekjear, 1984).

The noise in the electric field time series may be uncovered by subtracting the predicted time series $\mathcal{F}^{-1}(\mathbf{BZ})$, $\mathcal{F}$ being the Fourier transform from time to frequency domain. For this purpose the transfer function must be known for all Fourier coefficients which can be achieved by a polynomial approach to (3) or (4) (Larsen, 1989), an interpolation of band averaged values (Theissing, 1988) or values from stacked raw spectra (Clemens, 1993). Figure 9 gives an example of a periodic noise signal attributed to a pipeline (cf. Figure 2) which cannot be seen in the original time series. Obviously noise in the magnetic channel will yield a negative correlation between the difference field and $\mathbf{B}$. Theissing (1988) classifies noise according to various characteristics and is able to distinguish to a certain extent between noise in the magnetic and the electric field.

The remote reference technique (4) (cf. Gamble *et al.*, 1979) has become a powerful tool to counteract bias problems. However, great care is recommended in choosing the appropriate distance between local and remote site as this depends on the noise source characteristics, the conductivity structure and the frequency range under investigation. Whereas Goubau *et al.* (1984) found a separation of 200 m sufficient for periods beneath 10 s, Theissing (1988) and Jödicke and Grinat (1985) have observed a noise correlation scale of more than 50 km in the

pulsation range: Figure 10 presents simultaneous electromagnetic field records at four different sites being several ten kilometers apart. In the beginning of the record conspicuous similar signals appear at only two of the sites which are situated on more resistive subsurface while later a similar pattern can be detected at all four sites. Consequently the first signals are attributed to noise whereas the second are assumed to be of natural origin.

With respect to locally and remotely derived residuals $\mathbf{R}$ and $\mathbf{R}_r$ Larsen (1989) has presented necessary conditions on residuals for uncorrelated noise:

$$-\Gamma_N \leq \Re\Gamma \tag{5a}$$

$$-\Gamma_N \leq \Im\Gamma \leq \Gamma_N \tag{5b}$$

$$\Re\Gamma \leq \Lambda \leq 1/\Re\Gamma \tag{5c}$$

with $\Re\Gamma$ and $\Im\Gamma$ the real and imaginary part of $\Gamma$, $\Gamma = (\mathbf{R}^H\mathbf{R}_r)/\sqrt{(|\mathbf{R}|^2|\mathbf{R}_r|^2)}$, $\Lambda = |\mathbf{R}_r|/|\mathbf{R}|$, $\Gamma_N(\nu, p) = (1-p^{2/(\nu-2)})^{1/2}$, the last term being the $(1-p)$ level for the coherency of uncorrelated noise for $\nu$ degrees of freedom (Chave and Filloux, 1985). If (5a)–(5c) are valid for a given data set, the ratios

$$\Lambda_L = \frac{|\mathbf{R}|^2 - |\mathbf{E}_n|^2}{|\mathbf{E}_n|^2} = \frac{1}{\sqrt{\Lambda}\Re\Gamma} - 1 \tag{6a}$$

and

$$\Gamma_R = \frac{|\mathbf{R}_r|^2 - |\mathbf{E}_n|^2}{|\mathbf{E}_n|^2} = \frac{\sqrt{\Lambda}}{\Re\Gamma} - 1 \tag{6b}$$

reveal the influence of the different noise contributions. The various parameters are shown in Figure 11 yielding considerable change of noise contributions with frequency. The necessary conditions (5a–c) are met for almost all frequencies. For frequencies below 10 Hz the electric field noise dominates while the noise in the magnetic channels is larger for higher frequencies. As the magnetic noise between local and remote site seems to be uncorrelated, the remotely estimated impedance will be superior to the local estimates.

The minimization of bias and variance of the transfer functions estimates needs – beside the conventional time and frequency windowing procedures – the detection of suitable intervals of the time series due to the generally non-stationary noise and signal behaviour.

A number of coherence based selection schemes have been investigated by Travassos and Beamish (1988) who get their best results for single site data (cf. (3)) using the geometrical mean between the predicted and off-diagonal partial coherences as the selection criterium. If remote reference data are available they

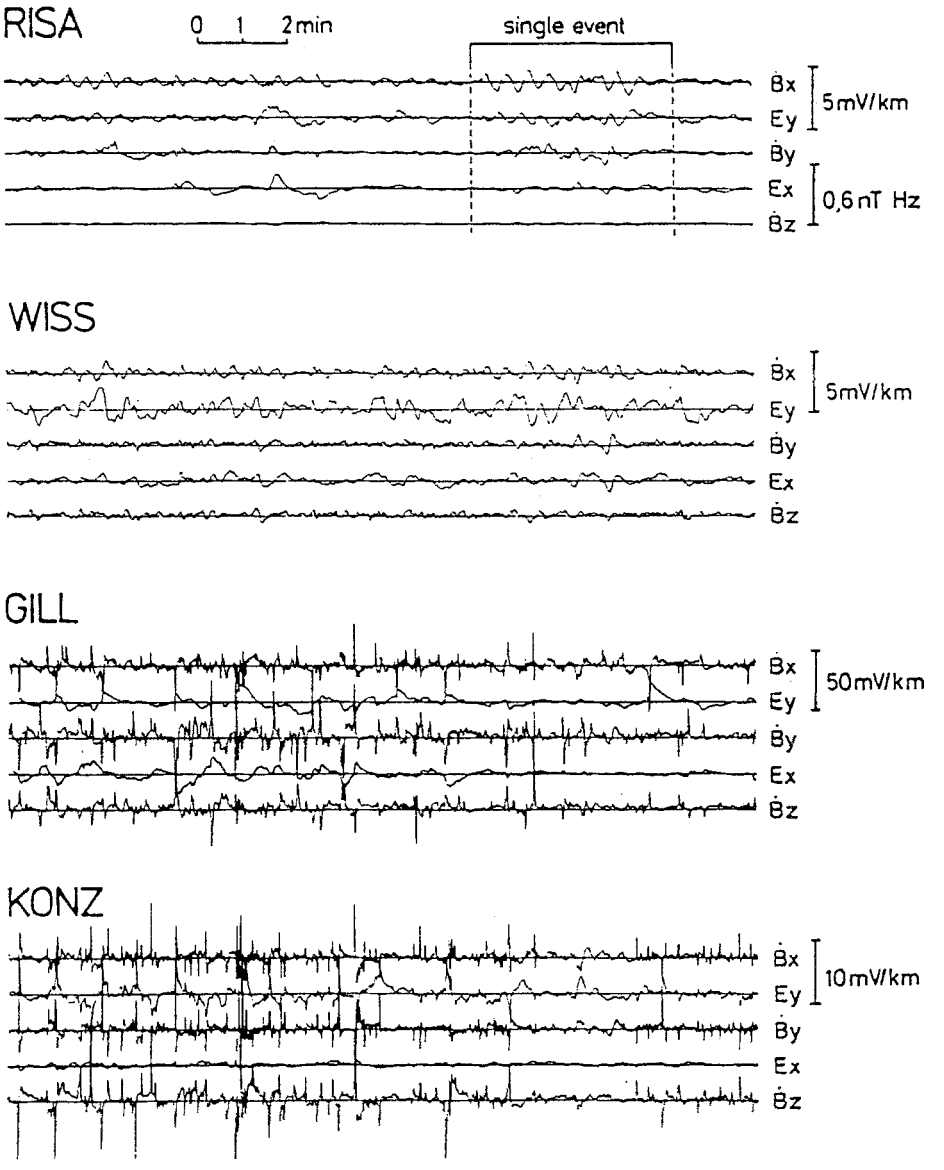


*Figure 10.* Noise correlation over large distances. Simultaneous record of the telluric and the time derivations of the magnetic field components at 4 sites in western and northern Germany (Jödicke and Grinat, 1985). The approximate distances between the sites are 40 km (RISA-WISS), 70 km (WISS-GILL), 40 km (GILL-KONZ). The first half of the time interval shows correlated noise in all channels only at the two bottom sites, while the second half reveals a similar signal pattern at all four sites which is attributed to natural origin.

favour the selection of intervals according to the remotely predicted coherence with subsequent single site processing.

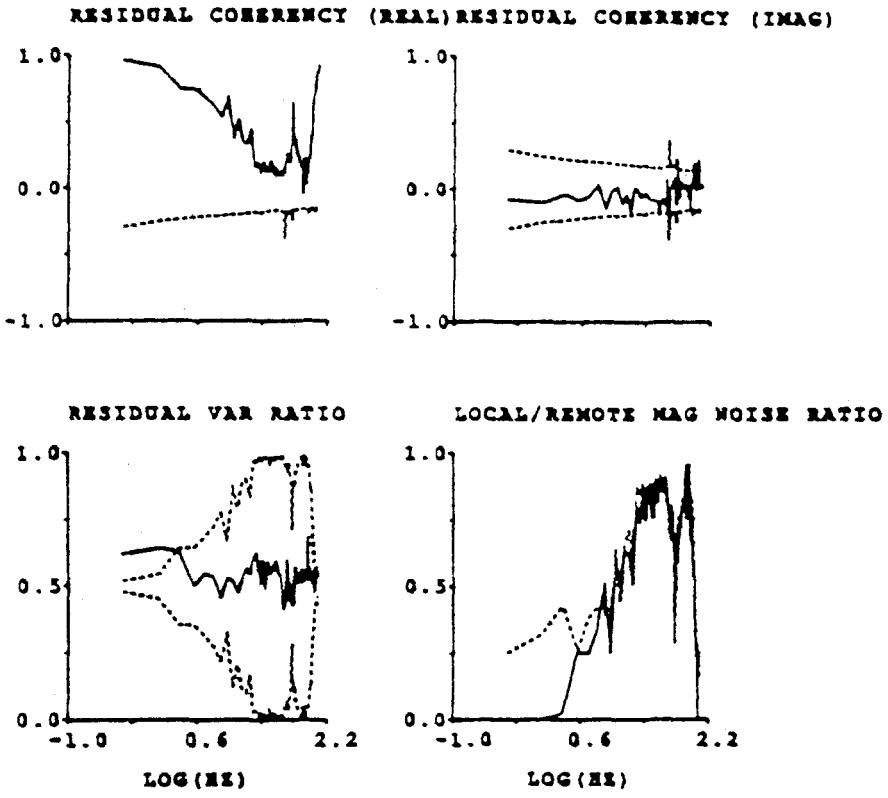


*Figure 11.* Uncorrelated noise test in the 0.1–100 Hz range (Larsen, 1989). Top left: $\Re\Gamma$ (solid) and $-\Gamma_n$ (dashed) according to (5a). Top right: $\Im\Gamma$ (solid) and $\Gamma_n$ (dashed) according to (5b). Bottom left: $\Lambda$ (solid) and $\Re\Gamma$ resp. $1/\Re\Gamma$ (dashed) according to (5c). Bottom right: Normalized local magnetic noise ratio $\Lambda_L/(1+\Lambda_L)$ (solid) and normalized remote magnetic noise ratio $\Lambda_R/(1+\Lambda_R)$ (dashed) (cf. (6a,b)).

Tzanis and Beamish (1989) use the Maximum Entropy spectral analysis method to gain high resolution transfer functions in the AMT range. Figure 12 compares their method to the conventional Fourier spectral analysis and exposes severe bias of the latter due to noise in narrow frequency bands. Although the computational effort of the Maximum Entropy algorithm is rather high and high frequency resolution is generally not needed in view of the smoothly varying form of transfer functions the algorithm might be a helpful diagnostic tool in the case of inscrutable situations.

A rather high time resolution is claimed by Chant and Hastie (1992, 1993) to be achieved by deriving time-frequency dependent spectral estimates

$$S(t,f) = \mathcal{F}(\Phi(-t,\tau) * C(t,\tau)), \tag{7}$$

where * represents a linear convolution in time $t$, $\Phi$ is a time lag kernel function and $C(t,\tau) = z_1(t+\tau/2)z_2(t-\tau/2)$ the bilinear cross power. The real signal

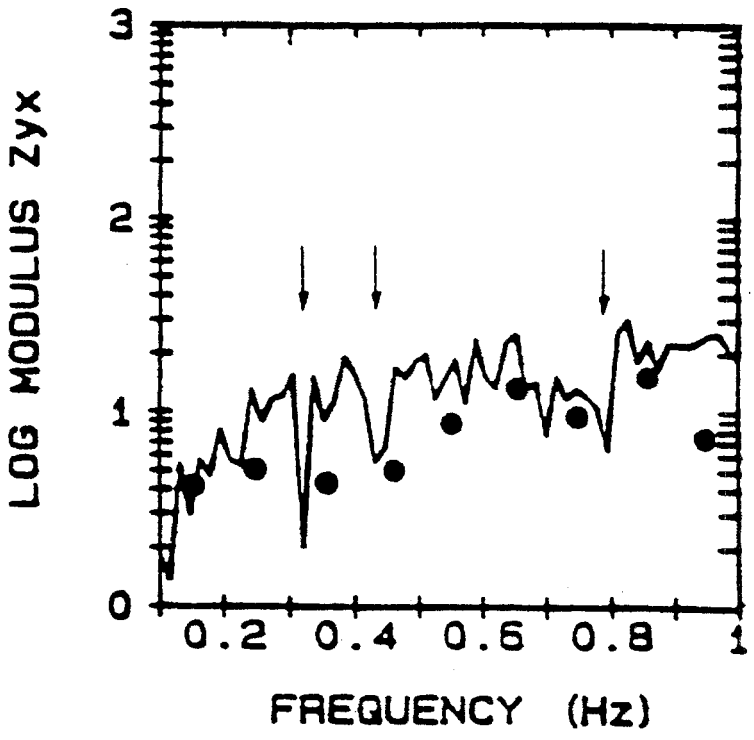


*Figure 12.* Comparison between Maximum Entropy spectral analysis method (solid line) and conventional Fourier analysis (dots) for the moduli of MT transfer function estimates (Tzanis and Beamish, 1989).

$x(t)$ is contained in $z = x + j\mathcal{H}(x)$ with $\mathcal{H}$ the Hilbert transform and $j$ the imaginary unit. The authors test various kernel functions and come to the conclusion that the MT impedance estimates are considerably non stationary. They try to eliminate the stationary part of the signal by taking the median of the $\Re \ln Z$ distribution and the mode of the impedance's phase distribution. The comparison with conventional robust procedures on the basis of a test data set (Jones *et al.*. 1989) reveals severe differences between the results (Figure 13). Consequently the authors fundamentally question the results from standard techniques commonly used in MT processing. However, such a severe conclusion demands a thorough comparison of methods with well defined artificial stationary and non-stationary noise and signal sources!

An overall improvement of the signal to noise ratio in the time series might be achieved by the previously mentioned data adaptive noise cancelling methods. This concept was originally developed by Widrow *et al.* (1975) and it was modified by Hattingh (1989) for MT processing. Figure 14 demonstrates the principle of the method: Primary and reference input $D$ and $X$ both contain correlated signal $S_0$ and $S_1$ and uncorrelated noise $n_0$ and $n_1$. The difference $\epsilon$ between the filtered signal

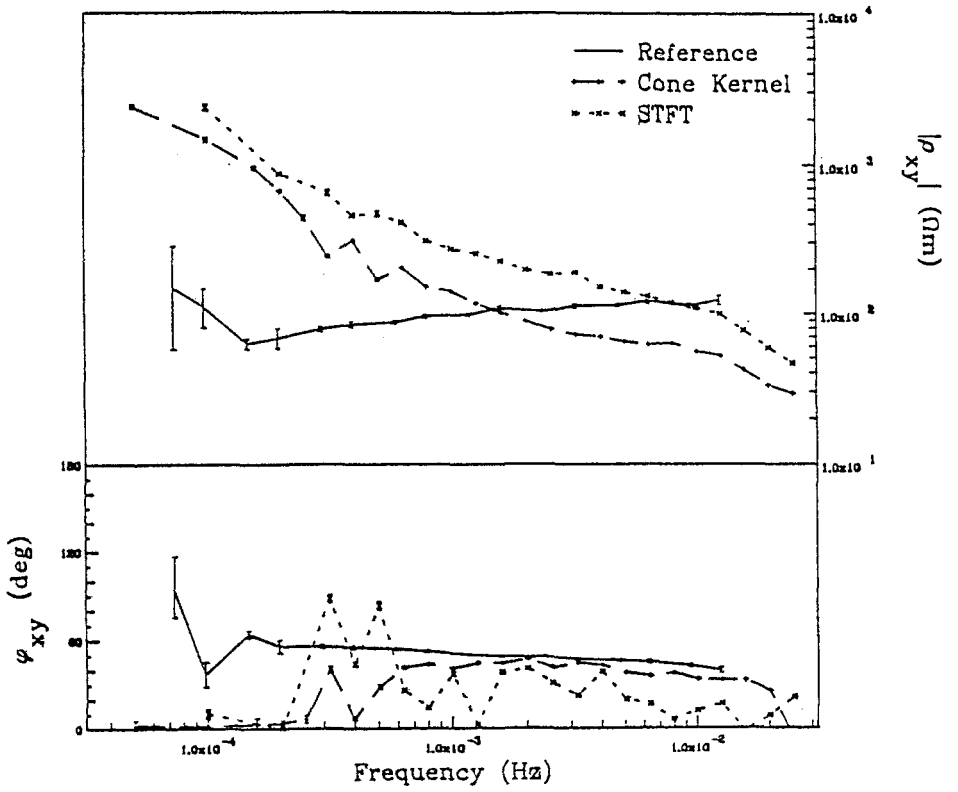


*Figure 13.* Comparison of transfer functions ($\rho_{xy}, \phi_{xy}$) estimated by time-frequency distribution analysis for different time-lag kernels (Cone kernel STFT) and conventional robust processing (Chant and Hastie, 1992).

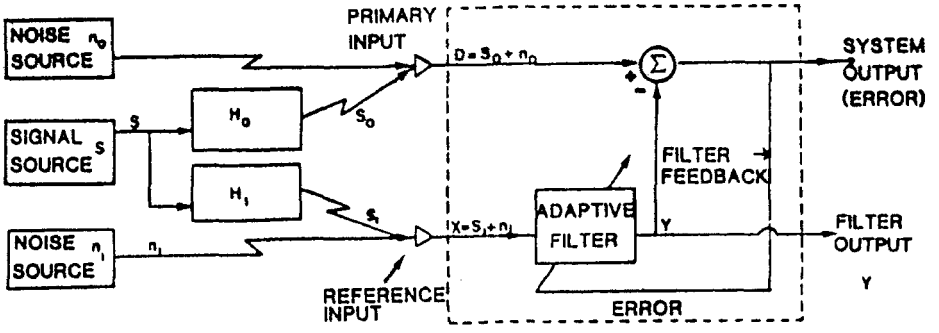


*Figure 14.* Correlated adaptive noise cancelling concept (Hattingh 1989).

$Y$ and $D$ is used to construct iteratively the filter weights $\mathbf{W} = (W_1, \ldots, W_L)$ by the Widrow-Hoff algorithm (Widrow *et al.*, 1975).

$$\mathbf{W}_{j+1} = \mathbf{W}_j + 2\mu\epsilon_j\mathbf{D}_j \tag{8}$$

$\mu$ denotes the gain constant and the subscript $j$ denotes the current iteration. Depending on the filter length $L$ and $\mu$ the filter may be "switched off" after a few iterations and only needs modification if the noise characteristics change. The input may be any of the observed electromagnetic field components either of a single or a remote site. The method is insensitive to moderate time lags between the time series. However, it is rather obscure to what extent the method also alters the original signal – a comparison with other techniques has yet to come!

### 3.3. Residual Distribution

So far the investigations have *a priori* assumed that the selected time windows would provide a subset of data with (a) identically and (b) independently distributed residuals which (c) obey a Gaussian distribution. Only under these three assumptions does the Gauss–Markov theorem guarantee the efficiency of the least squares regression estimate. For real data usually all three assumptions are violated. Thus least squares regression analysis has been generalized (Huber, 1981; Hampel *et al.*, 1986; Rousseeuw and Leroy 1987)) introducing the loss function $\rho(R)$ which has to be minimized

$$\sum_i \rho\left(\frac{R_i}{\sigma_i}\right) \stackrel{!}{=} \min . \tag{9}$$

$R_i$ is the $i$th element of **R** in (2) and $\sigma_i$ is its affiliated variance. For example for the conventional least squares regression analysis $\sigma_i$ = const. and $\rho(x) = |x|^2$! The minimum of (9) can be found by solving the system of equations with respect to the transfer functions **Z** of (2)

$$\sum_i w(R_i) R_i B_i = 0 \tag{10}$$

with the weight function $w(i) = \rho'(x)/x$ and $B_i$ the $i$th row of matrix **B** in (2). The solution $\hat{\mathbf{Z}}$ is called the regression $M$-estimate. As (10) is non-linear it has to be solved iteratively (cf. Egbert and Booker, 1986). It depends on $w(x)$ and the nature of **B** and **R** whether and how fast the iteration procedure converges. Table I lists several different weighting functions which are used either alone or in combined form. The HUBER-function is the only one in the list which theoretically guarantees convergence and it has a very high efficiency. However it descends rather slowly thus demanding a more rigorous suppression for large outliers, which is achieved by e.g. TUKEYS weight function. The last two weight functions are increasingly data adaptive. The THOMSON weight function results from empirical studies and adjusts to the number of data. Thus the descent of the weight function is controlled by the parameter $\alpha$ which is recommended to be equal to the $N$th quantile of the Normal distribution, $N$ being the number of residual data. LARSENs weight function $y(x)$ is derived from the distribution function of the actual residuals. It is

TABLE I
Weight functions $w(x)$ for M-regression analysis (cf. (10))

| | $w(x)$ | | Recommended threshold |
|---|---|---|---|
| HUBER | 1 | for $\|x\| \leq c$ | $c \approx 1.5$ |
| (Huber, 1964) | $\frac{1}{\|x\|}$ | for $\|x\| > c$ | |
| TUKEY | $\left(1 - \left(\frac{x}{c}\right)^2\right)^2$ | for $\|x\| \leq c$ | $3 < c < 9$ |
| (Beaton and Tukey, 1974) | 0 | for $\|x\| > c$ | |
| THOMSON (Thomson, 1977) | $\exp\{-e^{\alpha(\|x\|-\alpha)}\}$ | | $\alpha = Q_N$, (cf. text) |
| LARSEN | 1 | for $\|x\| < x_1$ | $x_1 = 0.7$ |
| (Larsen, 1989) | $y(x)$ | for $x_1 \leq \|x\| \leq x_2$ | (cf. text) |
| | 0 | for $x_2 < \|x\|$ | $x_2 \geq 2.6$ |

computationally expensive but offers the possibility of treating asymmetric residual distributions adequately.

Most authors recommend the use of the median as the initial robust estimator. As the solution of (10) is not scale invariant it requires the simultaneous robust estimation of scale. This is discussed theoretically by Huber (1981) and Hampel *et al.* (1986) and extensively with respect to applications in geophysics by Chave *et al.* (1987).

A rather powerful diagnostic tool provides the representation of the residuals in form of Q–Q (Quantile–Quantile) plots in which the ordered residuals are plotted against the quantiles of the assumed theoretical distribution. If the data behave according to the theory the graphs should approximate straight lines. Figure 15a demonstrates that the validity of the assumption may strongly depend on frequency while Figure 15b shows the impact of robust processing on the shape of the residual distribution. It is quite obvious that the graphic display offers great advantage compared to simple statistical tests such as the $\chi^2$-criterium.

Figure 16 compares the real part of the induction vector obtained by three different processing schemes. The robust scheme clearly produces the smoothest curves while the standard method suffers especially from severe bias.

### 3.4. LEVERAGING

The non-stationarity of signal variances may additionally aggravate the detection of outliers. On the one hand large signals may contain valuable information and provide a high signal to noise ratio, on the other hand they may contain a high amount of correlated noise and thus strongly mislead the estimation procedure. As the residual distribution is not sensitive to the leverage problem, a possible

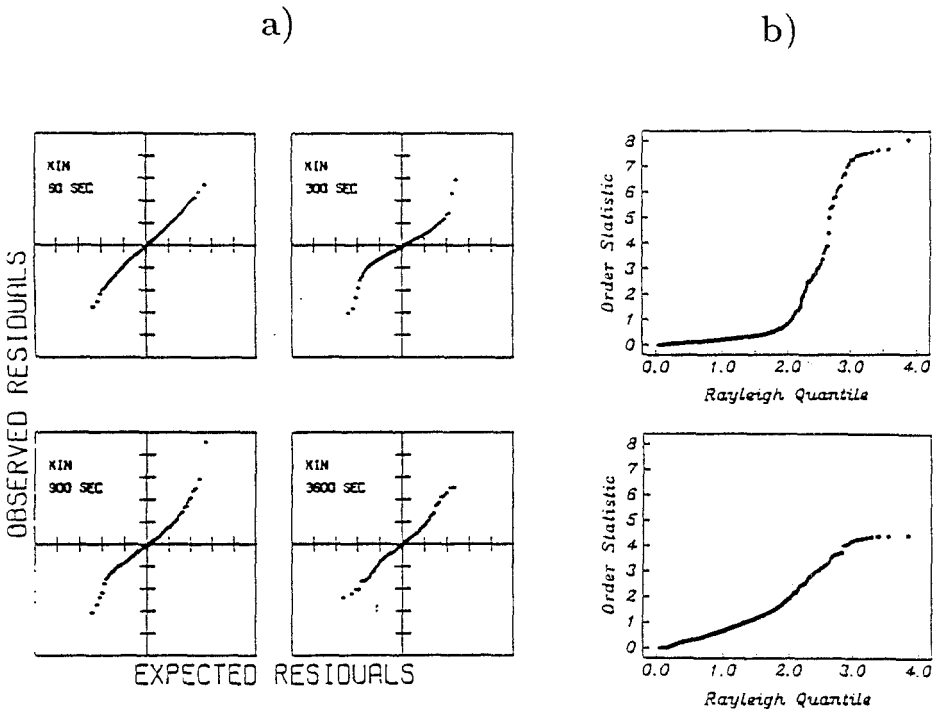


*Figure 15.* Q–Q plots of residuals. (a) Frequency dependence of GDS residual distribution. The heavy tails at intermediate periods indicate sporadic noise (Egbert and Booker, 1986). (b) Distribution of the MT residual magnitudes before and after robust processing (Chave and Thomson, 1989).

diagnostic tool is the hat matrix or information density matrix **H** (Hoaglin and Welsch, 1978),

$$\mathbf{H} = \mathbf{B}(\mathbf{B}^H\mathbf{B})^{-1}\mathbf{B}^H, \tag{11}$$

which projects the measured data **E** onto the predicted data **BZ**. The distribution of the diagonal elements of **H** may indicate leverage effects: If a diagonal element is equal to one the model is obviously completely determined by the corresponding datum and great caution is advised. Thus Chave and Thomson (1989) use the diagonal elements to discard conspicuous time segments. Figure 17b demonstrates that after the removal of leverage points the MT response function might get much smoother and less biased at the expense of a slight increase of the confidence limits.

### 3.5. Singular Value Decomposition

The bias problems of the least squares solution (2) have also been tackled by singular value decomposition (SVD) techniques (cf. Lawson and Hanson, 1974). For this purpose the matrix $\mathbf{A} = (\mathbf{B}, \mathbf{E})$ is formed. It contains all the measured

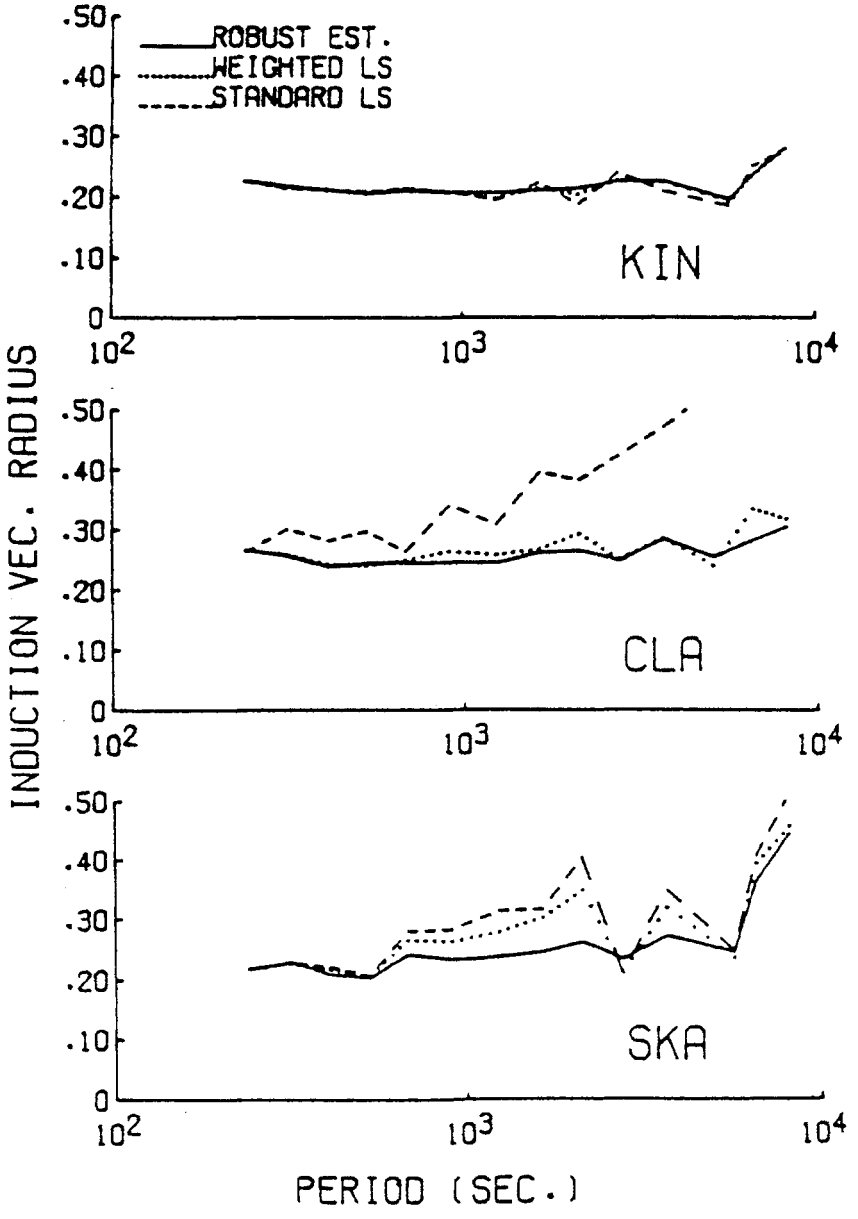


*Figure 16.* Comparison of three processing schemes for the real part of the induction vectors magnitude at three different sites (Egbert and Booker, 1986).

data and may be factorized into two orthonormal matrices **U** and **V** and a diagonal matrix $\Lambda$ containing the eigenvalues $\lambda_i$,

$$\mathbf{A} = \mathbf{U}\Lambda\mathbf{V}^H \tag{12}$$

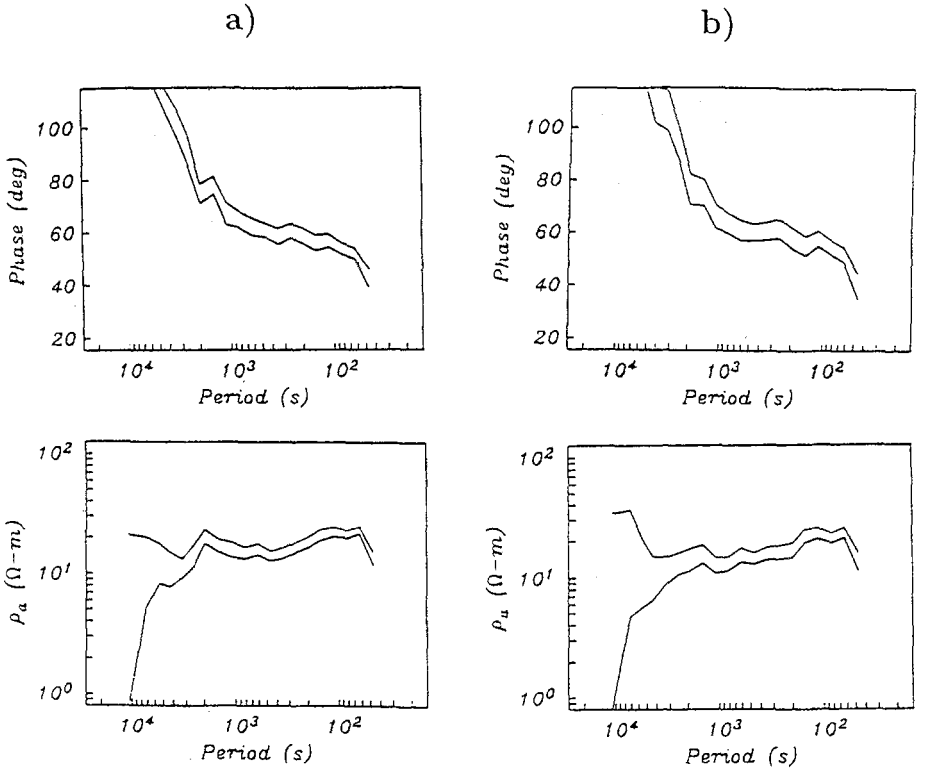


*Figure 17.* Comparison of $\rho_a$ and $\phi$ response functions before (a) and after (b) removal of leverage points (95% confidence limits) (Chave and Thomson, 1989).

Linear dependencies between the field components may be derived from the matrix **V** by treating the relative noise level of the electric and magnetic components as a free parameter. Park and Chave (1984) have calculated impedance estimates from that part of **V** which corresponds to the zero eigenvalues whereas Egbert and Booker (1989) have determined the impedance from the spectral density matrix

$$\mathbf{A}^H\mathbf{A} = \mathbf{V}\Lambda^2\mathbf{V}^H \tag{13}$$

This approach is computationally less expensive and it is extended by the authors to multivariate treatment of simultaneous measurements at different field sites. It involves the investigation of the source field structure and consequently allows for noise contributions due to a non-uniform source field.

A robust evaluation of (13) is described by Parr (1991) and performs rather well for extremely noisy data compared to a least squares robust regression analysis (Figure 18). For the frequencies above approx. 5 Hz the signal/noise ratio yields good data quality, the SVD analysis and the downward biased estimates being rather consistent. Obviously the noise is dominant in the electric field as the upward biased estimates of $\rho_a$ do not correspond to the phase behaviour. Below 1 Hz no interpretation is possible.

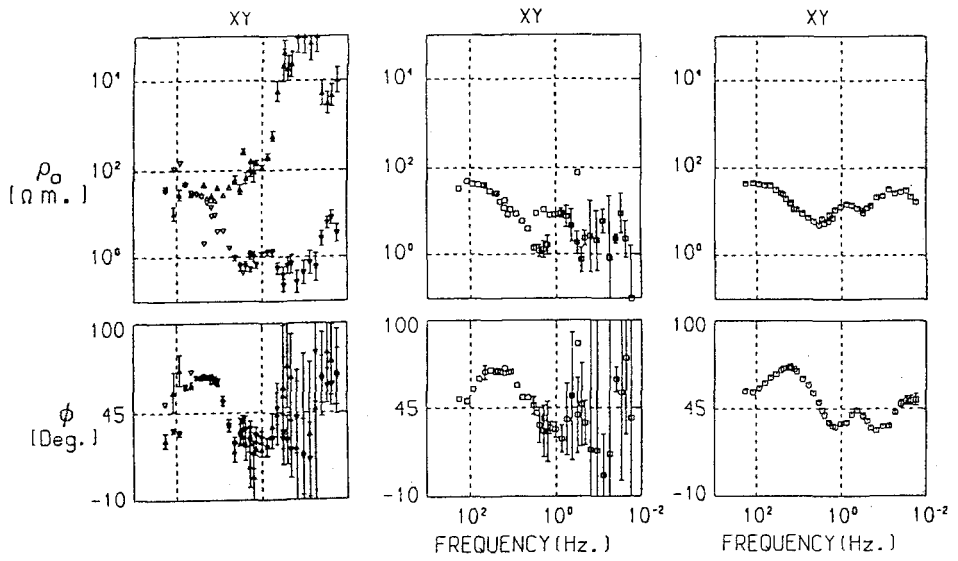


*Figure 18.* Comparison of robust least square technique according to (Chave and Thomson, 1989) and SVD analysis with a very noisy site (Parr, 1991). Transfer functions $\rho_a$ and $\phi$ in the frequency range between $10^{-2}$ and $10^2$ Hz. Left: Upward and downward biased estimates of the robust least squares technique. Center: Robust SVD analysis. Right: SVD analysis with constraints.

### 3.6. CONFIDENCE LIMITS

The estimation of confidence limits for the transfer function estimates depends on the noise distribution, the spectral covariance matrix and the number of degrees of freedom $\nu$. i.e. the number of statistically independent data. In the case of normally distributed residuals the previously mentioned textbooks discuss the construction of error boundaries in great detail. For the weighted parameter estimation Huber (1981, p.45) derives the asymptotic variance $\sigma_{R,\psi}$ of the residuals

$$\sigma^2_{R,\psi} = \frac{E\{\psi^2\}}{(E\{d\psi/dx\})^2} \tag{14}$$

with the expectation $E\{\ \}$, the influence function $\psi(x) = xw(x)$, $x$ the scaled residuum (cf. (9)) and $w(x)$ the weight function (cf. Table I). The estimation of $\nu$ is difficult and mostly based on assumptions about the white noise approximation of the residuals. As the $\chi^2$-distribution solely depends on $\nu$, Junge (1994) has derived estimates of $\nu$ under the assumption that the weighted residuals are roughly normally distributed and thus their squares follow a $\chi^2$ distribution. It has emerged that for both MT and GDS samples $\nu$ would fall below the number of the residuals by a factor of ten!

A distribution independent way of error estimation involves non-parametric statistics, of which the most frequently used is the jackknife method. It is treated

extensively and applied to a variety of spectral analysis methods by Thomson and Chave (1991) and especially for magnetotelluric response function estimates by Chave and Thomson (1989). The jackknife is based on the variance of sample subset estimates. Each subset is formed by leaving out in turn one datum $i$ and forming the subset estimates $\hat{x}_{-i}$. Thus the jackknife sample variance is (Chave and Thomson, 1989)

$$\hat{s}^2 = \frac{N-1}{N} \sum_i (\hat{x}_{-1} - \bar{x})^2 \tag{15}$$

where $\bar{x}$ is the arithmetic mean of the $\bar{x}_{-i}$. Confidence limits may be derived under very general conditions from the Student's $t$-distribution which for $\nu > 50$ can be approximated by the normal distribution. Complications occur in regression analysis as $\hat{s}$ will then become a covariance matrix and balance problems arise due to different variances of **E** and **B**. For further reading extensive literature is provided by Thomson and Chave (1991).

### 3.7. CONSTRAINTS

So far frequency bands have been treated independently permitting relatively free scattering of adjacent estimates. As in theory MT and GDS transfer functions vary smoothly with frequency it seems reasonable to put certain constraints on the variability of the estimates.

Fischer and Schnegg (1980) suggest the joint interpretation of $\rho_a$ and $\phi$ in view of the dispersion relations. The determination of bias and confidence limits, however, remains unclear.

A similar approach by Sutarno and Vozoff (1991) is based on regression M-estimation and the Hilbert transform and, in comparison with the response function in Figure 13 yields good agreement for central frequencies but shows considerable deviations at both ends of the analysed frequency range.

Instead of stacking weighted time sections Larsen (1975, 1980, 1989) processes the complete time series using a 1D model-supported polynomial presentation of the transfer-functions **Z** (3) resp. $\mathbf{Z}_r$ (4). As by this method the transfer functions are available over the whole frequency range, frequency and time domain residuals can be calculated from the measured and predicted data. An iterative robust processing scheme is applied until a normal distribution for the residuals in both domains is approximated. During the iterations a $D^+$ model is fitted to the data while the polynomials allow for deviations from the 1D model response. Figure 19 gives an example of time and frequency weights, the distribution of the weighted and unweighted time and frequency residuals and the estimated transfer functions. It shows that the downweighting is smeared over the time domain but it is dominant by a few large notches in the frequency domain. The weighted residuals approach a normal distribution rather well and the transfer functions are extremely smooth

due to the polynomial approach. However, the confidence intervals at different frequencies are not independent and the influence of the polynomial order is devious, thus the error information is distributed rather obscurely over the whole frequency range. An alternative could be the use of orthogonal polynomials suggested by Junge (1988), as then the polynomial coefficients as well as their confidence limits are estimated independently.

Yet another approach could be the smoothing by low order polynomials of immediately adjacent frequency estimates out of a limited frequency band. Parr (1991) combines this method with a 1D model constraint in a robust SVD analysis. Figure 18 shows the resulting extremely smooth response functions with very small error bars. With regard to the original low quality of the data the high resolution achieved is almost unbelievable. However, the comparison with an undisturbed field site in the vicinity of the disturbed one yielded very similar response functions except for the small bulge above 1 Hz which may very well be an artefact.

### 3.8. Comparison of Processing Techniques

An extensive comparison between 8 different processing algorithms (e.g. Law *et al.*, 1980; Jones *et al.*, 1983; Chave and Thomson, 1989; Jones and Jodicke, 1984; Egbert and Booker, 1986) is presented by Jones *et al.* (1989). It includes single site and remote reference observations, conventional and robust techniques applied to data from both magnetically active and magnetically quiet periods of 5 days duration, the sampling rate being 20 s. The time series data are available from the principal author on request. In this comparison at least robust methods perform best.

## 4. Conclusions

It has been pointed out that the treatment of time series in electromagnetic field studies is highly complicated and needs great skill. Especially measurements in industrialized and farming areas are frequently disturbed by man-made noise. Only in special cases can it easily be eliminated (e.g. the 16 2/3 and 50 Hz harmonics). Generally the noise variance varies with frequency, time and location and thus its source configuration often remains devious. The result may be uninterpretable data due to large bias effects and gross error bars.

Often even the careful selection of sites does not lead to the result hoped for while the application of the remote reference technique requires additional instrumental investment and, in special cases, even results in deterioration of the transfer function.

During the last decade sophisticated statistical methods have been developed to counteract these problems. They mostly treat the residuals resulting from the analysis of time series interrelations. Investigating the non-stationarity of noise,

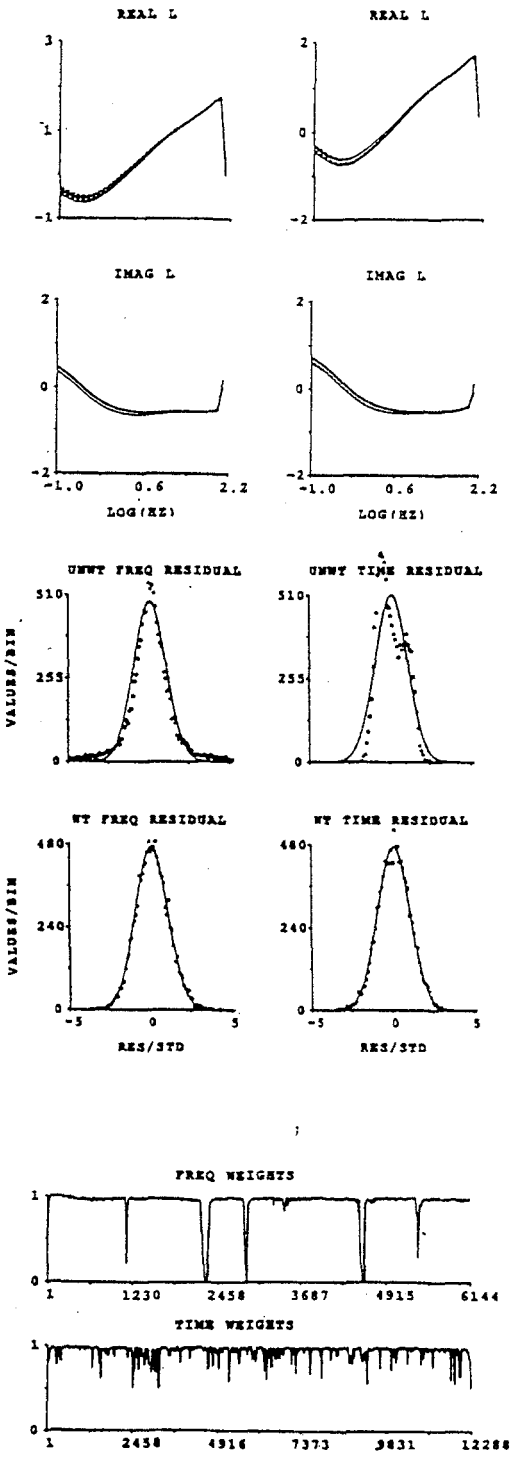


*Figure 19.* Polynomial presentation of transfer functions from a set of 12 288 data per time series sampled with 1/256 s (Larsen, 1989). Bottom: Time and frequency weights. Center: Distribution functions of unweighted and weighted time and frequency residuals. Top: Transfer function estimates – 95% confidence limits.

time segments of data are classified and – if necessary – downweighted using efficient weight functions. Thus bias and confidence limits can be remarkably reduced.

The signal is generally also non-stationary thus high energy events may dominate the estimation procedure. Leverage problems cannot be controlled by methods based on residual analysis but require the careful analysis of the information density matrix (hat matrix).

As the traditional estimation of confidence limits depends on both the distribution form and the number of degrees of freedom, parameter-free estimations such as the Jackknife are superior. However, they are computationally expensive.

Simultaneous estimation of transfer functions for different frequencies has led to the introduction of constraints, given by smoothness criteria, dispersion relations or some *a priori* information. The application of constrained processing schemes can achieve an enormous improvement of the transfer function quality but may in some cases result in loss of information or produce artefacts.

Simultaneous observations at different locations will yield most helpful information not only about noise but also about natural source field inhomogeneities which otherwise contribute to the residuals (Egbert, 1994). Correlated noise can be described by interstation transfer functions and thus be removed to estimate natural source transfer functions (Larsen *et al.*, 1994).

Using advanced processing techniques in the field the investigator nowadays can react very quickly to unexpected situations. In spite of the world-wide increasing noise level it should therefore be possible to obtain a rather dense net of high quality data. As most processing codes are widely accessible current problems are more related to availability of instruments, carrying out the measurements and reserving enough time for thorough data processing, best undertaken using several different techniques.

## Acknowledgements

I thank the committee of the working group I-2 of the IAGA for the invitation to give this review paper at the 12th Workshop of Induction in the Earth in Brest, France in 1994. Furthermore I am very grateful to all the authors who actively supplied me with their latest research work, to Dr. Rosemary Hutton who kindly read the manuscript several times and to Prof. Laust B. Pedersen for some useful comments.

## References

Ádám, A., Szarka, L., and Verö, J.: 1989, 'Natural and Man-made EM Variations in the Komló Coalfield', *Phys. Earth Planet. Int.* **53**, 207–213.

Ádám, A., Szarka, L., Verö, J., Wallner, A., and Gutdeutsch, R.: 1986, 'Magnetotellurics (MT) in Mountains – Noise, Topographic and Crustal Inhomogeneity Effects', *Phys. Earth Planet. Int.* **42**, 165–177.

Bartel, D. C. and Becker, A.: 1988, 'Time-domain Electromagnetic Detection of a Hidden Target', *Geophysics* **53**(4), 537–545.

Bartel, L. and Jacobson, R.: 1987, 'Results of a Controlled-source Audiofrequency Magnetotelluric Survey at the Puhimau Thermal Area, Kilauea Volcano, Hawaii', *Geophysics* **52**(5), 665–677.

Beaton, A. and Tukey, J.: 1974, 'The Fitting of Power Series, Meaning Polynomials, Illustrated on Band-spectroscopic Data', *Technometrics* **16**, 147–185.

Bendat, J. and Piersol, A.: 1971, *Random Data: Analysis and Measurement Procedures*, Wiley, New York.

Brasse, H.: 1993, 'Audiomagnetotellurische Tiefensondierungen in Nordost-Africa', *Diss. Fachb. Bergb. u. Geowiss*, TU Berlin.

Brasse, H. and Junge, A.: 1984, 'Einfluß erdmagnetischer Variationen auf den kathodischen Schutz von Rohrleitungen. *gwf gas/erdgas* **125**, 194–201.

Chant, I. and Hastie, L.: 1992, 'Time-frequency Analysis of Magnetotelluric Data', *Geophys. J. Int.* **111**, 399–113.

Chant, I. and Hastie, L.: 1993, 'A Comparison of the Stability of Stationary and Non-stationary Magnetotelluric Analysis Methods', *Geophys. J. Int.* **115**, 1143–1147.

Chave, A. and Filloux, J.: 1985, 'Observation and Interpretation of the Seafloor Vertical Electric Field in the Eastern North Pacific', *grl* **12**(12), 793–796.

Chave, A. and Thomson, D.: 1989, 'Some Comments on Magnetotelluric Response Function Estimation', *J. Geophys. Res.* **94**(B10), 14215-14225.

Chave, A. D., Thomson, D. J., and Ander, M. E.: 1987, 'On the Robust Estimation of Power Spectra, Coherences, and Transfer Functions', *J. Geophys. Res.* **92**(B1), 633–648.

Clemens, M.: 1993, 'Zur Beseitigung künstlicher Impulse in Zeitreihen erdmagnetischer und erdelektrischer Pulsationen', *Dipl. Arb. Inst. f. Geophys.* Univ. Göttingen.

Egbert, G.: 1994, 'Separating Signal from Noise Using Multiple-station MT Data', Paper presented at 12th Workshop on Electromagnetic Induction in the Earth, IAGA/IUGG, Brest, France, Aug. 8–13.

Egbert, G. and Booker, J.: 1989, 'Multivariate Analysis of Geomagnetic Array Data I: The Response Space', *J. Geophys. Res.* **94**, 14227–14247.

Egbert, G. D. and Booker, J. R.: 1986, 'Robust Estimation of Geomagnetic Transfer Functions', *Geophys. J. R. astr. Soc.* **87**, 173–194.

Filloux, J., Chave, A., Tarits, P., Petitt, R., Moeller, H., Dubreule, A., Petiau, G., and Banteaux, L.: 1994, 'Southeast Appalachians Experiment: Offshore Component', Paper presented at 12th Workshop on Electromagnetic Induction in the Earth.

Fischer, G. and Schnegg, P.-A.: 1980, 'The Dispersion Relations of the Magnetotelluric Response and Their Incidence on the Inversion Problem', *Geophys. J. R. astr. Soc.* **62**, 661–673.

Fontes, S., Harinarayana, T., Dawes, G., and Hutton, V.: 1988, 'Processing of Noisy Magnetotelluric Data Using Digital Filters and Additional Data Selection Criteria', *Phys. Earth Planet. Int.* **52**, 30–40.

Füllekrug, M.: 1994, 'Schumann-Resonanzen in den Magnetfeldkomponenten', Diss. mat. nat. Fak. Univ. Göttingen.

Gamble, T., Goubau., W., and Clarke, J.: 1979, 'Magnetotellurics with a Remote Magnetic Reference', *Geophysics* **44**(1), 53–68.

Goldstein, M. and Strangway, D.: 1975, 'Audio-frequency Magnetotellurics with a Grounded Electric Dipole Source', *Geophysics* **40**(4), 669–683.

Goubau, W. P. M. M., Koch, R., and Clarke, J.: 1984), 'Noise Correlation Lengths in Remote Reference Magnetotellurics', *Geophysics* **49**(4), 433–438.

Hampel, F. R., Ronchetti, E. M., Rousseeuw, P. J., and Stahel, W. J.: 1986, *Robust Statistics*, Wiley, New York.

Hattingh, M.: 1989, 'The Use of Data-adaptive Filtering for Noise Removal on Magnetotelluric Data', *Phys. Earth Planet. Int.* **53**, 239–254.

Hoaglin, D. and Welsch, R.: 1978, 'The Hat Matrix in Regression and ANOVA', *Am. Stat.* **32**, 17–22.

Huber, P. J.: 1964, 'Robust Estimation of a Location Parameter', *Ann. Math. Statist.* **35**, 73–101.
Huber, P. J.: 1981, *Robust Statistics*, Wiley, New York.
Jenkins, G. and Watts. P.: 1968, *Spectral Analysis and its Application*, Holden Day San Francisco.
Jödicke, H. and Grinat, M.: 1985, 'Magnetotelluric Measurements at the SE Flank of the Stavelot-Venn Anticline Using the Remote Reference Technique', *N. Jb. Geol. Paläont. Abh.* **171**(1–3), 425–440.
Jones, A., Chave, A., Egbert, G., Auld, D., and Bahr, K.: 1989, 'A Comparison of Techniques for Magnetotelluric Response Function Estimation', *J. Geophys. Res.* **94**(B10), 14201–14213.
Jones, A. and Jödicke, H.: 1984), 'Magnetotelluric Transfer Function Estimation Improvement by a Coherence-based Rejection Technique', Paper presented at 54th Annual International Meeting, Soc. of Expl. Geophys., Atlanta, Ga., Dec. 2–6.
Jones, A., Olafsdottir, B., and Tiikkainen, J.: 1983, 'Geomagnetic Induction Studies in Scandinavia – III. Magnetotelluric Observations', *J. Geophys.* **54**, 35–50.
Junge, A.: 1988, 'Analytical Presentation of Statistically Estimated Magnetotelluric Transfer Functions by a Set of Polynomials', *J. Geophys.* **62**, 193–197.
Junge, A.: 1990, 'A New Telluric KCL Probe Using Filloux's AgAgCl Electrode', *PAGEOPH* **134**(4), 589–598.
Junge, A.: 1994, 'Induzierte erdelektrische Felder- neue Beobachtungen in Norddeutschland und im Bramwald', Habil. Fachb. Physik Univ. Göttingen.
Larsen, J.: 1975, 'Low Frequency (0.1–6.0 cpd) Electromagnetic Study of Deep Mantle Electrical Conductivity Beneath the Hawaiian Islands', *Geophys. J. R. astr. Soc.* **43**, 17–46.
Larsen, J.: 1980, 'Electromagnetic Response Functions from Interrupted and Noisy Data', *J. Geomag. Geoelectr.* **32**, 89–103.
Larsen, J.: 1989, 'Transfer Functions: Smooth Robust Estimates by Least-squares and Remote Reference Methods', *Geophys. J. Int.* **99**, 645–663.
Larsen, J.: 1992), 'Transport and Heat Flux of the Florida Current at 27 N Derived from Cross-stream Voltages and Profiling Data: Theory and Observations', *Phil. Trans. R. Soc. Lond. A* **338**, 169–236.
Larsen, J., Mackie, R., Madden, T., Fiodelisi, A., Manzella, A., and Rieven, S.: 1994, 'Robust Processing for Removing Train Signals from Magnetotelluric Data in Central Italy', Paper presented at 12th Workshop on Electromagnetic Induction in the Earth.
Law, L., Auld, D., and Booker, J.: 1980, 'A Geomagnetic Variation Anomaly Coincident with the Cascade Volcanic Belt', *J. Geophys. Res.* **85**, 5297–5302.
Lawson, C. and Hanson, R.: 1974, *Solving Least Squares Problems*, Prentice-Hall, Englewood Cliffs, N.J.
Li, X. and Pedersen, L. B.: 1991, 'Controlled Source Tensor Magnetotellurics', *Geophysics* **56**(9), 1456–1461.
Macnae, J. C., Lamontagne, Y., and West, G.: 1984, 'Noise Processing Techniques for Time-domain EM Systems', *Geophysics* **49**(7), 934–948.
Masero, W. and Fontes, S.: 1992, 'Geoelectrical Studies of the Colônia Impact Structure', Santo Amaro, State of São Paulo, Brazil. *Revista Brasileira de Geofisica* **10**(1), 25–41.
Morat, P., Le Mouël, J.-L., and Granier, A.: 1994, 'Electrical Potential on a Tree. A Measurement of the Sap Flow?', *Sciences de la vie/Life sciences* **317**, 98–101.
Nichols, E., Morrison, H., and Clarke, J.: 1988, 'Signals and Noise in Measurements of Low-Frequency Geomagnetic Fields', *J. Geophys. Res.* **93**(B11), 13743–13754.
Ogunade, S.: 1986, 'Induced Electromagnetic Fields in Oil Pipelines Under Electrojet Current Sources', *Phys. Earth Planet. Int.* **43**, 307–315.
Olsen, K. B. and Hohmann, G. W.: 1992, 'Adaptive Noise Cancellation for Time-domain EM Data', *Geophysics* **57**(3), 466–469.
Otnes, R. K. and Enochson, L.: 1972, *Digital Time Series Analysis*, Wiley, New York.
Papoulis, A.: 1987, *Signal Analysis*, McGraw Hill, New York, 3rd edition.
Park, J. and Chave, A. D.: 1984, 'On the Estimation of Magnetotelluric Response Functions Using the Singular Value Decomposition', *Geophys. J. R. astr. Soc.* **77**, 683–709.
Parr, R.: 1991, 'Development of Magnetotelluric Processing and Modelling Procedures – Application to Northern England', Ph.D. Thesis, Fac. of Science, Univ. of Edinburgh.

Pedersen, L. and Svennekjear, M.: 1984, 'Extremal Bias Coupling in Magnetotellurics', *Geophysics* **49**(11), 1968–1978.

Petiau, G. and Dupis, A.: 1980, 'Noise, Temperature Coefficient, and Long-time Stability of Electrodes for Telluric Observations', *Geophys. Prosp.* **28**, 792–804.

Qian, W. and Boerner, D.: 1994, 'Electromagnetic Response of a Discretely Grounded Circuit; An Integral Equation Solution', *Geophysics* **59**(11), 1680–1694.

Qian, W. and Boerner, D.: 1995, 'Electromagnetic Modelling of Buried Line Conductors Using an Integral Equation', *Geophys. J. Int.* **121**(1), 203–214.

Qian, W and Pedersen, L.: 1991, 'Industrial Interference Magnetotellurics: An Example from the Tangshan Area, China', *Geophysics* **56**(2), 265–273.

Rousseeuw, P. and Leroy, A.: 1987, *Robust Regression and Outlier Detection*, John Wiley, New York.

Schnegg, P. and Fischer, G.: 1980, 'On-line Determination of Apparent Resistivity in Magnetotelluric Soundings', in V. Haak and J. Homilius (eds.), *Kolloquium Elektromagnetische Tiefenforschung Berlin-Lichtenrade*, pp. 173–184.

Sims. W., Bostick, F., and Smith, H.: 1971, 'The Estimation of Magnetotelluric Impedance Tensor Elements from Measured Data', *Geophysics* **36**(5), 938–942.

Spies, B. R.: 1988, 'Local Noise Prediction Filtering for Central Induction Transient Electromagnetic Sounding', *Geophysics* **53**(8), 1068–1079.

Stephan, A. and Strack, K.-M.: 1991, 'A Simple Approach to Improve the S/N Ratio for TEM Data Using Multiple Receivers', *Geophysics* **56**(6), 863–869.

Strack, K.-M., Hanstein, T., and Eilenz, H.: 1989, 'LOTEM Data Processing for Areas with High Cultural Noise Levels', *Phys. Earth Planet. Int.* **53**, 261–269.

Sutarno, D. and Vozoff, K.: 1991, 'Phase-smoothed Robust M-Estimation of Magnetotelluric Impedance Functions', *Geophysics* **56**(12), 1999–2007.

Szarka, L.: 1988, 'Geophysical Aspects of Man-made Electromagnetic Noise in the Earth – A Review', *Surv. in Geophys.* **9**, 287–318.

Theissing, J. T.: 1988, Eine Methode zur Trennung von Signal- und Störanteilen in magnetotellurischen Zeitreihen, Dipl. Arb. Inst. für Geophysik Univ. Münster.

Thomson, D.: 1977, 'Spectrum Estimation Techniques for Characterization and Development of WT4 Waveguide, I', *Bell Syst. Tech. J.* **56**, 1769–1815.

Thomson, D. J. and Chave, A. D.: 1991, 'Jackknifed Error Estimates for Spectra, Coherences, and Transfer Functions', In S. Haykin (ed.), *Advances in Spectrum Analysis and Array Processing, Vol. 1*, Chapter 2, Prentice Hall.

Travassos, J. and Beamish, D.: 1988, 'Magnetotelluric Data Processing – A Case Study', *Geophys. J. R. astr. Soc.* **93**, 377–391.

Tzanis, A. and Beamish, D.: 1989, 'A High-resolution Spectral Study of Audiomagnetotelluric Data and Noise Interactions', *Geophysical Journal* **97**, 557–572.

Widrow, B., Glover Jr., J., McCool, J., Kaunitz, J., Williams, C., Hearn, R., Zeidler, J., Dong Jr., E., and Goodin, R.: 1975, 'Adaptive Noise Cancelling: Principles and Applications', *Proc. Inst. Elect. Electron. Eng.* **63**, 1692–1716